nature nanotechnology

ARTICLES

PUBLISHED ONLINE: 9 MAY 2010 | DOI: 10.1038/NNANO.2010.82

Dispensing nano–pico droplets and liquid patterning by pyroelectrodynamic shooting

P. Ferraro*, S. Coppola, S. Grilli*, M. Paturzo and V. Vespini

Manipulating and dispensing liquids on the micrometre- and nanoscale is important in biotechnology and combinatorial chemistry, and also for patterning inorganic, organic and biological inks. Several methods for dispensing liquids exist, but many require complicated electrodes and high-voltage circuits. Here, we show a simple way to draw attolitre liquid droplets from one or multiple sessile drops or liquid film reservoirs using a pyroelectrohydrodynamic dispenser. Local pyroelectric forces, which are activated by scanning a hot tip or an infrared laser beam over a lithium niobate substrate, draw liquid droplets from the reservoir below the substrate, and deposit them on the underside of the lithium niobate substrate. The shooting direction is altered by moving the hot tip or laser to form various patterns at different angles and locations. Our system does not require electrodes, nozzles or circuits, and is expected to have many applications in biochemical assays and various transport and mixing processes.

Modifying the wetting properties of hydrophobic surfaces using electric fields (known as electrowetting)[1] or displacing liquid droplets using heat gradients (thermocapillarity)[2] are useful processes in microfluidic and optofluidic systems for adapting the shape of liquid menisci and patterning liquids or forming and displacing droplets[3–18]. Highly integrated 'lab-on-a-chip' devices for biochemical assays use microfluidic systems that rely on these processes to manipulate liquid flows into micro-channels[19–21]. Recently, 'digital microfluidics', which use single droplets to confine reactions[22–27], have been proposed as an alternative approach to liquid flow systems. In this approach, open structures allow droplet microreactors to be dispensed onto two-dimensional chips and to be displaced subsequently by acoustic waves or by electrowetting to avoid fluidic connections[23,24]. This operation depends on precise and reliable droplet dispensers, the simplest of which involve liquids flowing through a cylindrical tube[28] or heat ejection of droplets from nozzles[29].

Different dispensing methods have been developed in recent years. For example, stationary liquid microjets dispense droplets by inducing fluid interface instabilities[30], whereas atomic force microscope probes dispense nanolitre droplets through an aperture in their apex[14,31]. Other approaches make use of electrohydrodynamic jetting[32], which involves a tube with a meniscus bearing a Taylor cone profile spraying a fine jet. On-demand droplets with sizes much smaller than that of the delivery nozzle have been obtained by pulsed electrohydrodynamic liquid jetting[33,34]. High-resolution electrohydrodynamic jet printing (below the limit of commercial thermal or piezoelectric inkjet printers, which produce 10–20-pl droplets and linewidths down to 50 μm) has been achieved using microcapillary nozzles[13]. Drop-on-demand printing of conductive ink has been obtained by the application of electrostatic fields[7]. Electric-field-induced formation of micro- and nanolitre droplets has also been used for manipulating biomolecules[14]. All these electrohydrodynamic techniques provide submicrometre droplets and have the flexibility to pattern fragile organics or biological materials that are incompatible with conventional methods such as photolithography. However, dispensing liquids for biochemical analysis or patterning requires the arrangement of appropriate electrodes and the use of high-voltage circuits between the liquid reservoir and the receiver substrate, which can be cumbersome. Moreover, the capillary nozzles require complicated fabrication procedures and may be subject to cross-contamination.

Here, we present a new concept of electrohydrodynamic-based droplet generation called pyroelectrohydrodynamic shooting, for the direct drawing and dispensing of droplets with volumes on the scale of attolitres and radii as low as ∼300 nm from liquid drops or film reservoirs. This technique does not require electrodes, high-voltage circuit connections or special capillary nozzles. The electric fields are generated pyroelectrically using functionalized substrates of lithium niobate (LN). The pyroelectric effect has been used recently for wettability patterning[35], particle trapping[36] and liquid microlenses[37–39]. Here, we use this effect to transfer liquids between two substrates and manipulate the droplets three-dimensionally. The simplicity of the technique suggests potential uses in a range of liquid manipulation fields, such as generating and dispensing daughter droplets, fragmenting microlitre drops, and liquid printing. We expect the technique to have many applications in biochemistry and nano-printing.

Design and working principle of the dispenser

Our system consists of two plates and a heat source. The heat source could be a non-contact infrared beam (continuous-wave CO_2 laser emitting at 10.6 μm) or a hot tip of a conventional soldering iron, acting as a contact stimulus (Fig. 1a,b). A microscope glass slide forms the base of the liquid reservoir (which could be a drop or a film), and the LN crystal wafer (z-cut, optically polished and 500 μm thick) acts as an auxiliary plate that drives the process and acts as a substrate for the dispensed liquids (see Methods for more details). A pointwise thermal stimulus is applied to the LN crystal to induce the pyroelectric effect locally. The maximum operation temperature of the hot tip is ∼250 °C.

At equilibrium, the spontaneous polarization P_s of the LN crystal is fully compensated by the external screening charge, and no electric field exists[40]. According to the pyroelectric effect, the temperature change ΔT causes a variation ΔP_s, which builds up an electric potential across the z surfaces. Neglecting the losses, a surface charge density $\sigma = P_c \Delta T$ appears locally when the tip heats the crystal,

CNR Istituto Nazionale di Ottica–Sezione di Napoli Via Campi Flegrei, 34–80078 Pozzuoli (Napoli), Italy. *e-mail: pietro.ferraro@ino.it; simonetta.grilli@ino.it

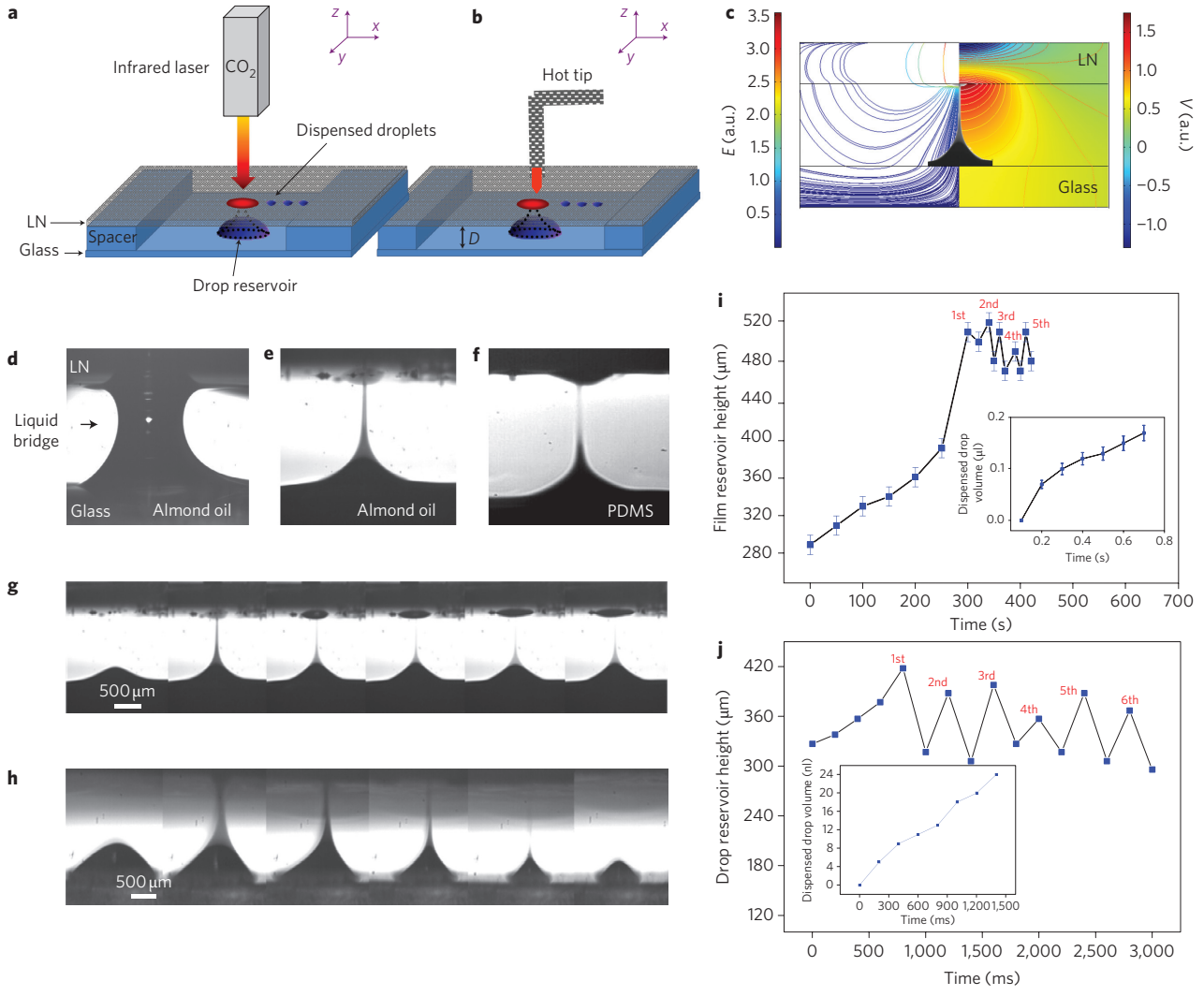

Figure 1 | Pyroelectrohydrodynamic dispenser. a,**b**, Schematic of the microfluidic system consisting of two plates and a heat source (an IR laser or hot tip of a conventional soldering iron). **c**, Three-dimensional axially symmetric plot of the electric field lines (left) and electric potential (right) obtained using the finite-element method. **d**, Liquid bridge obtained when D is shorter than the critical distance; equation (1). **e**,**f**, Shooting of almond oil and PDMS (PDMS has a continuous blasting cone due to its higher viscosity). **g**,**h**, Sequence of almond oil shots taken from a film stimulated by hot tip (**g**) and from a sessile drop stimulated by IR laser (**h**). **i**,**j**, Plot of temporal height variation of the film (**i**) and drop (**j**). Single shots are detectable. Insets: plots of the corresponding volume transfer rate.

where P_c is the pyroelectric coefficient ($P_c = -8.3 \times 10^{-5}$ C m^{-2} °C^{-1} for LN @ 25 °C). The electric field exerts an attractive force on the liquid (Fig. 1c) and, when sufficiently strong, deforms the liquid into a conical tip from which thin liquid jets are released. Such a liquid tip is similar to the Taylor cone[13–15], but differs because the liquid is not conductive.

It is well known that for a fixed drop volume, a critical value D_c can be defined for the distance D between the base and the substrate, according to the following expression[41]:

$$D_c = (1 + \theta/4)V^{1/3} \quad (1)$$

where θ is the contact angle and V is the volume of the drop reservoir. A stable liquid bridge establishes when $D < D_c$ (Fig. 1d). The most relevant case here refers to $D > D_c$, when a stable liquid bridge cannot be established between the plates, and a liquid streaming regime occurs (Fig. 1e,f). We use such instability to break up the liquid reservoir and to dispense droplets. Figure 1g,h shows two sequences of liquid shooting in which nanolitre and picolitre almond oil droplets were dispensed from a liquid film and from a sessile drop reservoir stimulated by the hot tip and by infrared laser pulses (power, 10 W; length, 100 ms), respectively. The phenomena were captured by a CMOS-camera with a recording frame rate of 125 frame s^{-1} (Supplementary Movies S1,S2). The dynamic evolutions show that the reservoir first deforms into a conical tip, with a height that increases under the pyroelectrohydrodynamic force, and then behaves as a 'dispensing gun' that blasts droplets periodically until the electric field vanishes. Figure 1i,j shows the temporal height variation of the film and drop reservoirs (main plots), respectively, and the volume transfer rates (insets) corresponding to the sequences in Fig. 1g,h. The film dispensed 160 nl after 5 shots with a period of 100 ms and a rate of 30 nl per shot, whereas the drop dispensed 164 nl after 55 shots with a period of 200 ms and a rate of ~3 nl per shot. Figure 1h shows that the initial volume (180 nl) of the drop reservoir was reduced to ~16 nl after 55 shots (last frame in Fig. 1h).

It is important to note that electrohydrodynamics-based liquid emissions have been deeply investigated theoretically for a wide variety of configurations (liquids flowing in capillary tubes or

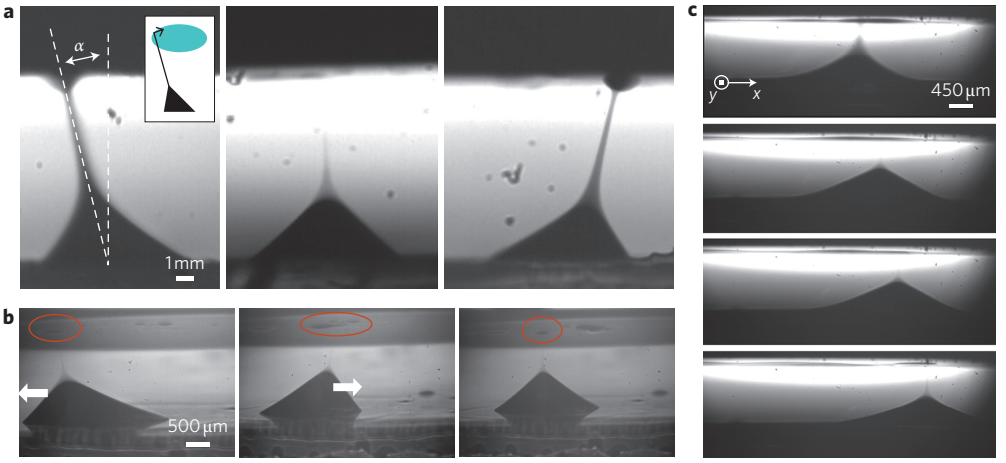

Figure 2 | Functionalities of the dispensing gun. a, Shooting of nanolitre almond oil droplets within a solid angle (off-axis directions up to ~20°) from a standing sessile drop by moving the hot tip. The liquid was deposited over an area of ~23 mm^2. **b**,**c**, Shooting of almond oil droplets to different locations from a sessile drop (**b**), which is induced to translate onto the PDMS-coated glass by moving the hot tip beyond the threshold angle, and from a film (**c**), where the dispensing gun moves more easily and in two dimensions. A lateral displacement of 1.6 mm along the *x*-axis is visible between the first (top) and last frames (bottom), and the translation of ~1 mm along the *y*-axis is noticeable through the variation in image focus (**c**).

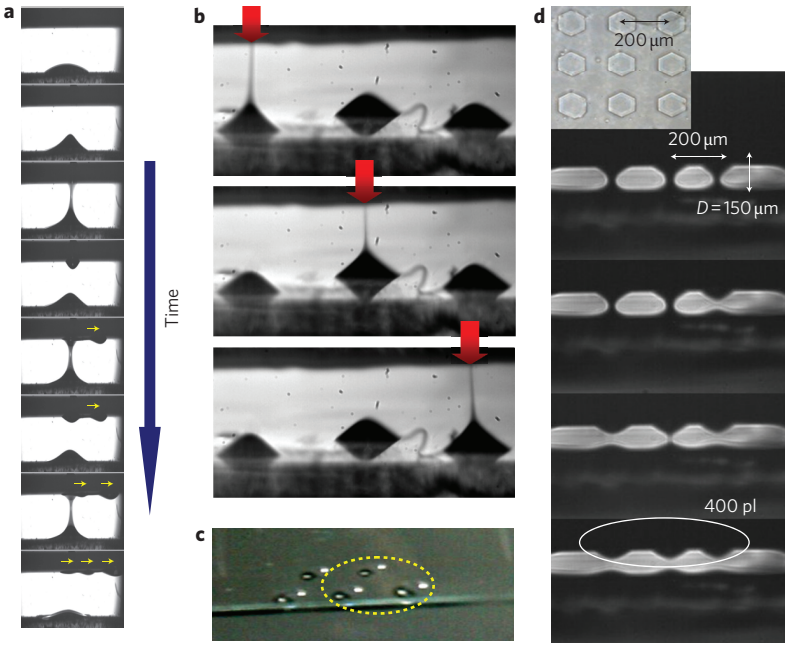

Figure 3 | Additional functionalities. a, Sequential images of the dispensing and successive lateral sliding of nanolitre droplets. The hot tip was positioned closer to the edge of the LN plate, where the glass spacer favoured thermal dissipation and generated colder regions (right side in the picture) where the dispensed droplets slid by thermocapillarity. **b**, Sequential activation of three different drop reservoirs by the precise spatial scanning of the infrared laser beam. **c**, Perspective image of five almond oil sessile drops on PDMS-coated glass, where the circle indicates the drops activated in **b. d**, Simultaneous dispensing of ~400-pl droplets of PDMS in correspondence with the ordered reversed domains of a 200-µm periodically poled LN wafer.

nozzles, tip streaming from liquid films, steady cone jets, co-flowing liquids and so on; see refs 1−6 in Supplementary Information S3), and different scaling laws have been proposed, even with reciprocal discrepancies. Only recently, Basaran's group[15] presented a comprehensive physics picture of electrohydrodynamic tip streaming (cone formation, jet emission and break-up) from a liquid film of finite conductivity, even though the process is well known and has been used for decades. Simulations and experiments reported therein were related to an axially symmetric case. Conversely, the electrohydrodynamic dispenser proposed here is based on liquid emission from sessile drops, and a well established theory is not yet available. In fact, the fluid physics does not differ from standard electrohydrodynamics applied to pendant and sessile droplets[42,43]. Moreover, the value of the electric field obtained in pyroelectrohydrodynamics for a ΔT of 100 °C (~10 kV) is comparable to the values (900 V to 24 kV) usually adopted in electrohydrodynamics experiments for inkjet printing[7,13] (Supplementary Information S1).

Functionalities of the dispenser

The pyroelectrohydrodynamic 'dispensing gun' may operate with various functionalities. For example, the shooting direction can be changed within a wide solid angle (Fig. 2a) by moving the thermal source (hot tip or laser beam). In fact, the regions with highest electric fields follow the thermal source displacement. The

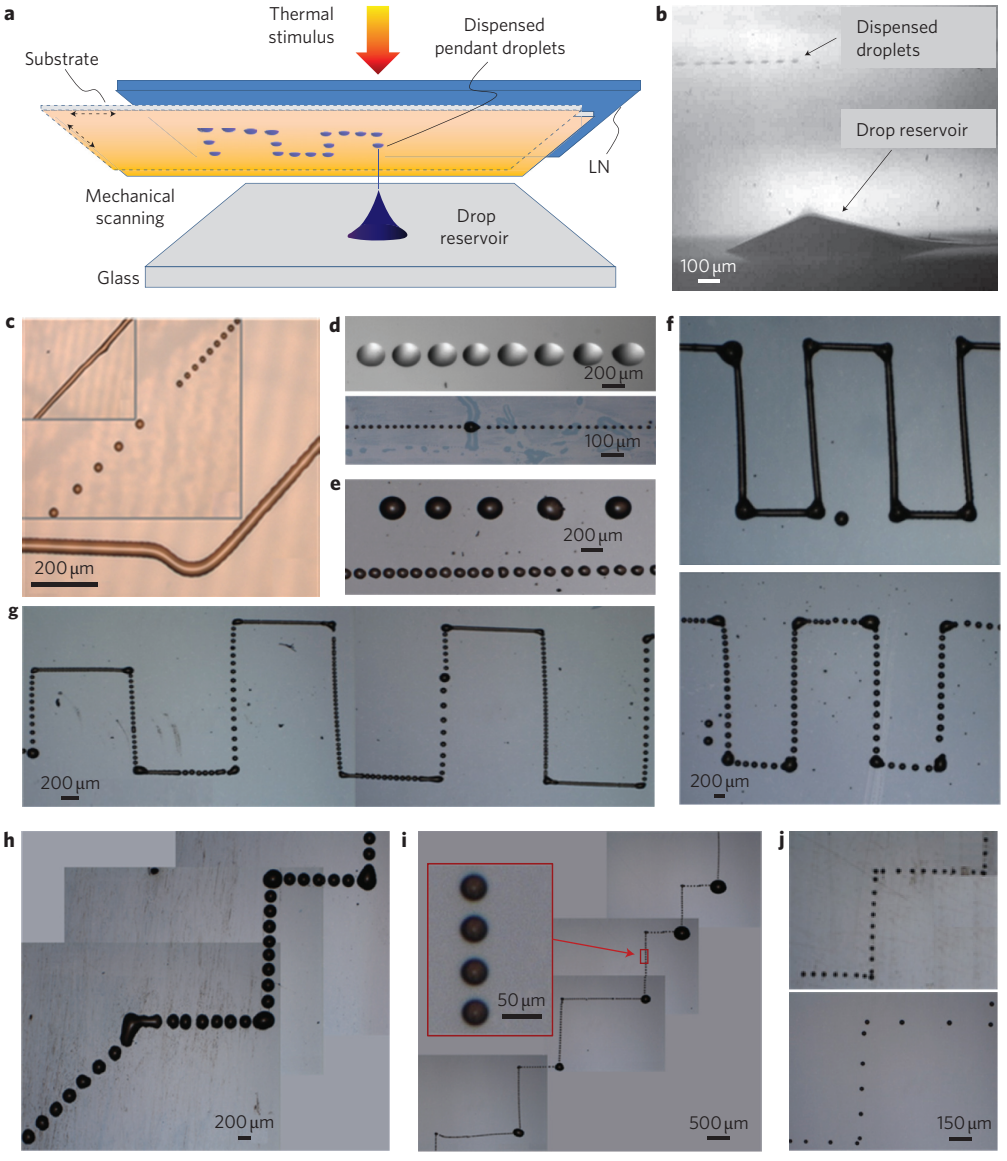

Figure 4 | Dispensing nanolitre droplets for liquid patterning. a, Liquid is dispensed onto a translating substrate inserted between the LN and the glass plate. **b**, Side view of the typical printing functionality. **c**, Simple patterns printed by oleic acid: separate droplets (diameters, 40 and 25 μm), straight and curved lines (width, 40 μm). **d**, Linear array of periodic separate droplets printed by almond oil (top) and mineral oil (bottom) (diameter, 15 μm). **e**, Two parallel printed lines obtained using two different adjacent drop reservoirs. **f**, Continuous (top) and dotted (bottom) Greek fret printed by mineral oil. **g**, Continuous and dotted patterned Greek fret. **h**, Dotted staircase including a non-orthogonal angle. **i**, Staircase with smaller droplets (25 μm) printed with large vertices. **j**, Dotted staircase with small vertices (droplet diameter, 30 μm).

off-axis shooting angles reach values up to ~20°, allowing the dispenser to deposit liquids onto an area of ~23 mm^2 from a standing drop reservoir. Larger angles induce the drop reservoir to translate during shooting and dispense to different locations (drop in Fig. 2b and film in Fig. 2c). The drop reservoir moves only beyond a certain threshold angle (Supplementary Movie S3). In fact, when the drop undergoes the maximum asymmetrical deformation under the off-axis electric force, the solid – liquid surface tensions are no longer balanced and a resulting force moves the drop (Fig. 2b). Such imbalance of surface tensions is similar to that induced by a thermal gradient in thermocapillarity. The dispensing gun moves more easily in the case of the film reservoir (Fig. 2c), because no solid – liquid interface tension prevents movement of the blasting cone. The sequence of images in Fig. 2c shows the translation of the dispensing gun up to 1.6 mm (x-axis) and 1 mm (y-axis) (Supplementary Movie S4) during shooting.

The shooting function can also be synchronized harmonically with the displacement of the droplets while they are dispensed continuously (Fig. 3a; see also Supplementary Movie S5). The sequence of images in Fig. 3a shows the formation of three droplets sliding to the right side. Such droplets could be collected and managed into a microfluidic system. This function is implemented by positioning the hot tip closer to the edge of the LN plate where the thermal dissipation, favoured by the contact with the glass spacer (see Fig. 1b), generates colder regions. The 'dispensing and sliding effect' is driven by electrohydrodynamics (dispensing of droplets) and thermocapillarity[2] (sliding of droplets to colder regions) activated simultaneously by a single external stimulus.

The infrared laser beam offers several advantages over the hot tip. The temperature gradient induced by the laser can be varied quantitatively by modulating the laser power, and it is spatially highly selective. Beam focusing allows one to control and reduce the area

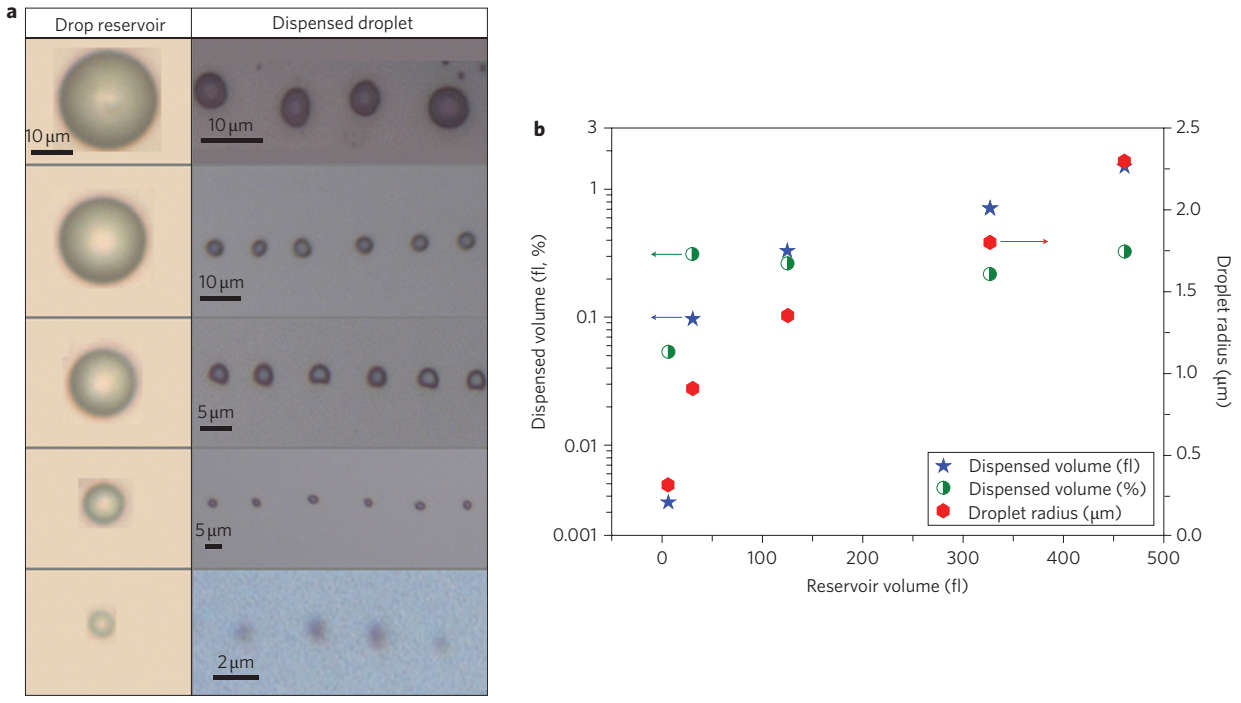

Figure 5 | Nanoscale droplets. a, Optical microscope images of different drop reservoirs and corresponding dispensed tiny droplets of oleic acid. **b**, Corresponding volume and radius values of the dispensed droplets versus those of the reservoir (the left *y*-scale is logarithmic).

to be stimulated (Supplementary Information S1). Figure 3b,c shows side and perspective views of three drop reservoirs stimulated selectively and sequentially by the laser beam (red arrows, Fig. 3b). The laser beam can be split into different directions to achieve simultaneous and parallel blasting from multiple guns for high-throughput dispensing processes.

A different experiment was performed using a LN wafer functionalized through a periodically poled structure[44] to demonstrate the possibility of dispensing picolitre droplets to specific locations. The LN structure consisted of a square array of hexagonal regions with reversed polarization (see Methods), and the base was spin-coated with a layer of polydimethylsiloxane (PDMS). The thermal stimulus enabled the formation of three droplets in correspondence with the hexagons, with a lateral separation of 200 μm. Liquid filaments and unstable liquid bridges[41] were formed due to the higher viscosity of the PDMS fluid (Fig. 3d). In fact, the separation distance D was ~150 μm and therefore shorter than the critical value given by equation (1). The results show that 400-pl pendant droplets were dispensed (Supplementary Movie S6) after the bridges collapsed.

Liquid nanoprinting and patterning

These results show the possibility of drawing and dispensing liquid samples from a drop or film reservoir onto a functionalized substrate such as LN, with intriguing functionalities. However, the deposition of droplets directly onto the warm LN wafer causes spreading of the liquid (more visible in Fig. 1g and Supplementary Movies S3,S4) due to the electrowetting effect caused by the uncompensated charges generated pyroelectrically on the crystal surface (Supplementary Information S2). Moreover, the deposition of droplets onto chips other than the LN plate is desirable. The pyroelectrohydrodynamic dispenser was therefore improved according to the scheme presented in Fig. 4a (see Methods and Supplementary Movies S7–S11). The new configuration allowed the dispensing gun to print different liquid patterns consisting of separate droplets (with different distances and periods) and/or continuous lines by controlling the translation direction and speed of the substrate. Figure 4b shows a side view of the droplet dispensing onto the moving substrate. Figure 4c presents typical simple patterns printed by a carboxyl acid based liquid (oleic acid), consisting of straight and curved continuous lines (width, ~40 μm) and separate droplets of different sizes (40 and 25 μm) and periods. Figure 4d shows periodic droplets printed by almond oil (up) and mineral oil (bottom), with diameters of ~200 and 15 μm, respectively. More complex patterns have been printed by mineral oil, including a continuous and dotted Greek fret (Fig. 4e), a Greek fret with combined continuous and dotted lines (Fig. 4f), a dotted staircase including a non-orthogonal angle (Fig. 4g), a dotted staircase with smaller droplets (diameter, ~25 μm), in which the larger vertices were obtained by stopping the substrate during dispensing (Fig. 4h), and a dotted staircase with further droplets and small vertices (droplet diameter, ~30 μm; Fig. 4i).

Another intriguing functionality of the printing process consists in the simultaneous streaming of adjacent drop reservoirs with different volumes by the same thermal stimulus. A sort of multi-dispensing process is obtained that leads to the formation of parallel lines of droplets of two different diameters (Fig. 4j).

It is important to point out that the technique is able to print droplets with much reduced dimensions by decreasing the volume of the drop reservoir (for example, after a certain number of shots). Figure 5a presents optical microscope images of tiny droplets of oleic acid dispensed from drop reservoirs of various volumes and dimensions (Fig. 5b). The smallest dispensed droplets have volumes as low as ~3.6 al and radii of ~300 nm.

All these results demonstrate the ability of the pyroelectrohydrodynamic dispenser to print liquid droplets and lines with highly regular diameters and widths and according to a wide variety of geometries. To the best of our knowledge, the droplets printed here have sizes comparable to those obtained recently by an electrohydrodynamic approach[13]; in that case, however, special nozzles and high-voltage electrodes and circuits were used. They are also comparable to those shown in ref. 31, where, however, special atomic force microscope probes were designed and used.

The pyroelectrohydrodynamic dispenser presented here may find applications in the field of biochemical assays, because it can

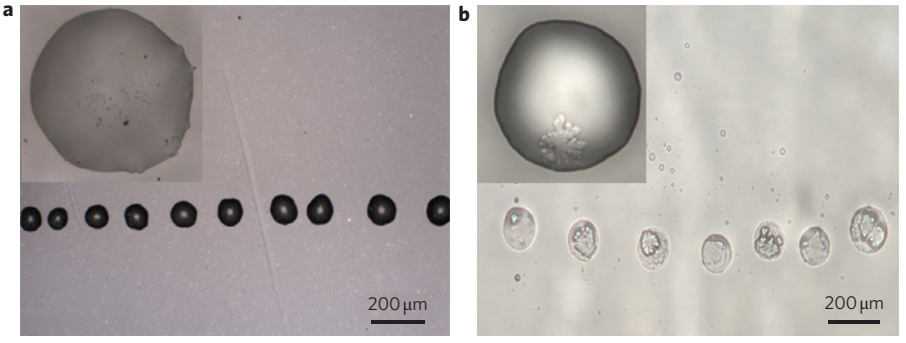

Figure 6 | Daughter droplets of specific suspensions. a,**b**, Optical microscope images of dispensed droplets containing carbon nanotubes dispersed in mineral oil (**a**) and cell cultivation medium mixed with oleic acid, where typical salt crystallization is visible (**b**).

break up parent drops containing special materials dispersed into an oil phase. In fact, the compartmentalization of individual samples in droplets dispersed in an oil phase is becoming a powerful method for high-throughput assays in chemistry and biology[45,46]. For example, Fig. 6a shows dispensed daughter droplets of carbon nanotubes dispersed in mineral oil, and Fig. 6b shows the daughter droplets of a sample of cell cultivation medium mixed with carboxyl oil.

Additional experiments were performed to characterize the most relevant key attributes of the approach for different fluids (Supplementary Information S3). The revolutionary feature of the pyroelectrohydrodynamic dispenser would be to avoid the use of the drawing and delivery instruments traditionally used in biochemical protocols (that is, syringes, nozzels), thus making the assay procedures much easier and faster. In fact, the pyroelectrohydrodynamic dispenser would be used as a tool for breaking up parent drops that are standing on a surface into daughter droplets to be delivered directly to the desired substrate, where the droplets could be used as reaction confinements for biochemical assays and also for single-cell analysis[28,47].

Conclusion

In conclusion, we have developed a pyroelectrohydrodynamic droplet dispenser based on pyroelectric forces. Our system offers several advantages over conventional electrohydrodynamic systems. It does not require electrodes or special circuits and no sample pre-treatments are therefore required. The system is easy to use and non-invasive, and is therefore potentially useful as a portable instrument for *in situ* drawing and delivering of liquid samples within a chip. Furthermore, because it does not require nozzles, issues of cross-contamination can be avoided. The possibility of simultaneous shooting adjacent drop reservoirs would enable high-throughput biochemical assays, and the development of integrated platforms for parallelized reactors and compartments for spatially separated processes. The 'sliding droplet' function can easily mix and transport tiny droplets rapidly, and the ability to print attolitre droplets may be useful for single-cell analysis.

Methods

Lithium niobate crystal. The uniform spontaneous polarization of commercially available *z*-cut LN crystals can be reversed by electric field poling[45] for fabricating periodically poled LN crystals. An external voltage exceeding the coercive field of the material (~21 kV mm^{-1}) is required to reverse the orientation of the ferroelectric domains, and inversion selectivity is usually ensured by an appropriate resist pattern generated by photolithography. The upper image in Fig. 3d shows the optical microscope image of a periodically poled LN sample fabricated in our laboratory by the electric field poling. The sample consists of a square array of bulk reversed domains with a period ~200 μm along both *x*- and *y*-directions. The sign of the pyroelectric coefficient is reversed according to the inverted ferroelectric domains[40].

Infrared laser. A continuous-wave CO_2 laser emitting at a wavelength of $\lambda = 10.6$ μm, with a power of 10 W, was used in this work. The emission power was modulated in the interval 0–100% by an external voltage ranging from 0 to 5 V. The output laser beam had a diameter of 4 mm and was focused by an appropriate lens to obtain the desired focal spot dimension down to the diffraction limit of about a half-wavelength (5 μm). The laser was mounted onto an *x*–*y* translation stage and the laser head was ~25 cm away from the LN wafer.

Hot tip source. The hot tip of a conventional soldering iron was used as contact thermal stimulus. The diameter of the tip was 1 mm and the maximum operation temperature was 250 °C. The temperature of the substrate was measured by a thermocouple device.

Set-up and preparation of the reservoirs. The base was a conventional 1-mm-thick microscope glass slide. In the case of Figs 1– 3, thin spacers were glued on the edges of the base to superimpose the LN plate at a fixed distance of ~1 mm. In Figs 4–6, the base glass slide and the auxiliary LN plate were mounted on two independent vertical translation stages to control the reciprocal distance *D*. A resist spin-coated cover glass, mounted on a computer-controlled *x*–*y* translation stage (speed, ~700 μm s^{-1}), was inserted in between, and acted as the substrate on which the droplets were dispensed. Different techniques were adopted for preparing the film and drop reservoirs:

(1) Almond oil as liquid film. Drops a few micolitres in volume were deposited onto a solvent-cleaned glass substrate, and a conventional spin-coater was used to obtain a uniform thin layer of oil (Figs 1e,1g,1i,2c refer to these experiments).
(2) Almond oil as sessile drop on clean glass. An appropriate electronic syringe was used to deposit the drops directly onto the surface of the solvent-cleaned glass slide (Figs 2a,3a refer to these experiments).
(3) Almond oil as sessile drop on PDMS coated glass. In this case the base glass slide was spin-coated with a PDMS (Sylgard 184) layer by a spin-coater (60 s at 5,000 rpm). The link process in PDMS was obtained by thermal curing for 10 min at 100 °C on a hotplate. One or more drops of different volumes (depending on the specific experiment) were successively deposited onto the surface of the cured PDMS (Figs 1h,1j,2b,3b,3c,4b refer to these experiments).
(4) PDMS on glass. Drops a few micolitres in volume were deposited onto a solvent-cleaned glass substrate and a conventional spin-coater was used (5 s at 1,000 rpm) to obtain a uniform thin layer of PDMS (Figs 1f,3d refer to these experiments).
(5) Oleic acid alone (Figs 4c,4j,5) and with cell cultivation medium (EMEM + 2 mM glutamine + 10% fetal bovine serum) as a sessile drop on a glass slide coated with a layer of cured PDMS (Fig. 6b).
(6) Mineral oil (Sigma Aldrich) alone (Fig. 4d (bottom), 4e–i) and with carbon nanotubes (multiwalled, diameter 110–170 nm, length 5–9 μm, Aldrich Chemistry) as a sessile drop on a glass slide coated with a layer of cured PDMS (Fig. 6a).

Imaging set-up. The measurement equipment consisted of a white-light-emitting lamp, a neutral density filter and an imaging lens to visualize the cone formation and droplet ejection onto a fast CMOS camera. This camera was able to capture 125 frame s^{-1} with a resolution of 1,280 × 1,024 pixel^2 and pixel area of 12 × 12 μm^2. Two lenses with different focal lengths *f* and magnifications M were used to investigate the dynamics of the process: $f = 100$ mm, M = 1.4 and $f = 25.4$ mm, M = 2.2 for infrared and hot tip stimuli, respectively.

Received 21 December 2009; accepted 25 March 2010; published online 9 May 2010

References

1. Mugele, F. & Baret, J.-C. Electrowetting: from basics to applications. *J. Phys. Condens. Matter* **17,** R705–R774 (2005).
2. Jiao, Z., Huang, X., Nguyen, N.-T. & Abgrall, P. Thermocapillary actuation of droplet in a planar microchannel. *Microfluid. Nanofluid.* **5,** 205–214 (2008).

3. Squires, T. M. & Quake, S. R. Microfluidics: fluid physics at the nanoliter scale. *Rev. Mod. Phys.* **77,** 977–1026 (2005).
4. Gallardo, B. S. *et al.* Electrochemical principles for active control of liquids on submillimeter scales. *Science* **283,** 57–60 (1999).
5. Kataoka, D. E. & Troian, S. M. Patterning liquid flow on the microscopic scale. *Nature* **402,** 794–797 (1999).
6. Aronov, D., Rosenman, G., Karlov, A. & Shashkin, A. Wettability patterning of hydroxyapatite nanobioceramics induced by surface potential modification. *Appl. Phys. Lett.* **88,** 163902 (2006).
7. Whitesides, G. M. The origins and the future of microfluidics. *Nature* **442,** 368–373 (2006).
8. Velev, O. D., Prevo, B. G. & Bhatt, K. H. On-chip manipulation of free droplets. *Nature* **426,** 515–516 (2003).
9. Choi, J. *et al.* Drop-on-demand printing of conductive ink by electrostatic field induced inkjet head. *Appl. Phys. Lett.* **93,** 193508 (2008).
10. Choi, W.-K. *et al.* Nano-liter size droplet dispenser using electrostatic manipulation technique. *Sens. Actuat. A* **136,** 484–490 (2007).
11. Lee, J.-G. *et al.* Electrohydrodynamic (EHD) dispensing of nanoliter DNA droplets for microarrays. *Biosens. Bioelectron.* **21,** 2240–2247 (2006).
12. Strobl, C. J., von Guttenberg, Z. & Wixforth, A. Nano- and pico-dispensing of fluids on planar substrates using SAW. *IEEE Trans. Ultrason. Ferroelectr. Freq. Control* **51,** 1432–1436 (2004).
13. Ahmed, R. & Jones, T. B. Optimized liquid DEP droplet dispensing. *J. Micromech. Microeng.* **17,** 1052–1058 (2007).
14. de Heij, B. *et al.* Highly parallel dispensing of chemical and biological reagents. *Anal Bioanal Chem.* **378,** 119–122 (2004).
15. Park, J. U. *et al.* High-resolution electrohydrodynamic jet printing. *Nature Mater.* **6,** 781–789 (2007).
16. Loha, O. Y. *et al.* Electric field-induced direct delivery of proteins by a nanofountain probe. *Proc. Natl Acad. Sci. USA* **105,** 16438–16443 (2008).
17. Collins, R. T., Jones, J. J., Harris, M. T. & Basaran, O. A. Electrohydrodynamic tip streaming and emission of charged drops from liquid cones. *Nature Phys.* **4,** 149–154 (2008).
18. Barrero, A. & Loscertales, I. G. Micro- and nanoparticles via capillary flows. *Annu. Rev. Fluid Mech.* **39,** 89–106 (2007).
19. Marchand, G., Delattre, C., Campagnolo, R., Pouteau, P. & Ginot, F. Electrical detection of DNA hybridization based on enzymatic accumulation confined in nanodroplets. *Anal. Chem.* **77,** 5189–5195 (2005).
20. Manz, A. & Becker, H. *Microsystem Technology in Chemistry and Life Sciences* (Springer, 1998).
21. Bruin, G. J. Recent developments in electrokinetically driven analysis on microfabricated devices. *Electrophoresis* **21,** 3931–3951 (2000).
22. Taniguchi, T., Torii, T. & Higuchi, T. Chemical reactions in microdroplets by electrostatic manipulation of droplets in liquid media. *Lab Chip* **2,** 19–23 (2002).
23. Pollack, M. G., Shenderov, A. D. & Fair, R. B. Electrowetting-based actuation of droplets for integrated microfluidics. *Lab Chip* **2,** 96–101 (2002).
24. Cho, S. K., Moon, H. & Kim, C. J. Creating, transporting, cutting and merging liquid droplets by electrowetting-based actuation for digital microfluidic circuits. *J. Microelectromech. Syst.* **12,** 70–80 (2003).
25. Schaerli, Y. & Hollfelder, F. The potential of microfluidic water-in-oil droplets in experimental biology. *Mol. BioSyst.* **5,** 1392–1404 (2009).
26. Hung, L. H. *et al.* Alternating droplet generation and controlled dynamic droplet fusion in microfluidic device for CdS nanoparticle synthesis. *Lab Chip* **6,** 174–178 (2006).
27. Guttenberg, Z. *et al.* Planar chip device for PCR and hybridization with surface acoustic wave pump. *Lab Chip* **5,** 308–317 (2005).
28. Basaran, O. A small-scale free surface flows with breakup: drop formation and emerging applications. *AICHE J.* **48,** 9 (2002).
29. Suryo, R. & Basaran, O. A. Dripping of a liquid from a tube in the absence of gravity. *Phys. Rev. Lett.* **96,** 034504 (2006).
30. Casner, A. & Delville, J.-P. Laser-induced hydrodynamic instability of fluid interfaces. *Phys. Rev. Lett.* **90,** 144503 (2003).
31. Ondarcuhu, T. *et al.* Controlled deposition of nanodroplets on a surface by liquid nanodispensing: application to the study of the evaporation of femtoliter sessile droplets. *Eur. Phys. J. Special Topics* **166,** 15–20 (2009).
32. Cherney, L. T. Structure of Taylor cone-jets: limit of low flow rates. *J. Fluid Mech.* **378,** 167–196 (1999).
33. Chen, C.-H., Saville, D. A. & Aksay, I. A. Scaling laws for pulsed electrohydrodynamic drop formation. *Appl. Phys. Lett.* **89,** 124103 (2006).
34. Chen, A. U. & Basaran, O. A. A new method for significantly reducing drop radius without reducing nozzle radius in drop-on-demand drop production. *Phys. Fluids* **14,** L1–L4 (2002).
35. Ferraro, P., Grilli, S., Miccio, L. & Vespini, V. Wettability patterning of lithium niobate substrate by modulating pyroelectric effect to form microarray of sessile droplets. *Appl. Phys. Lett.* **92,** 213107 (2008).
36. Grilli, S. & Ferraro, P. Dielectrophoretic trapping of suspended particles by selective pyroelectric effect in lithium niobate crystals. *Appl. Phys. Lett.* **92,** 232902 (2008).
37. Miccio, L. *et al.* Tunable liquid microlens arrays in electrode-less configuration and their accurate characterization by interference microscopy. *Opt. Express* **17,** 2487–2499 (2009).
38. Grilli, S. *et al.* Liquid micro-lens array activated by selective electrowetting on lithium niobate substrates. *Opt. Express* **16,** 8084–8093 (2008).
39. Miccio, L., Paturzo, M., Grilli, S., Vespini, V. & Ferraro, P. Hemicylindrical and toroidal liquid microlens formed by pyro-electro-wetting. *Opt. Lett.* **34,** 1075–1077 (2009).
40. Rosenblum, B., Bräunlich, P. & Carrico, J. P. Thermally stimulated field emission from pyroelectric $LiNbO_3$. *Appl. Phys. Lett.* **25,** 17–19 (1974).
41. Maeda, N., Israelachvili, J. N. & Kohonen, M. M. Evaporation and instabilities of microscopic capillary bridges. *Proc. Natl Acad. Sci. USA* **100,** 803–808 (2003).
42. Wohlhuter, F. K. & Basaran, O. A. Shapes and stability of pendant and sessile dielectric drops in an electric field. *J. Fluid Mech.* **235,** 481–510 (1992).
43. Harris, M. T. & Basaran, O. A. Equilibrium shapes and stability of nonconducting pendand drops surrounded by a conducting fluid in an electric field. *J. Colloid Interface Sci.* **170,** 308–319 (1995).
44. Ferraro, P., Grilli, S. & De Natale, P. *Ferroelectric Crystals for Photonic Applications, Including Nanoscale Fabrication and Characterization Techniques*, Series in Materials Science, Vol. 91 (Springer, 2008).
45. Taly, V., Kelly, B. T. & Griffiths, A. D. Droplets as microreactors for high-throughput biology. *ChemBioChem* **8,** 263–272 (2007).
46. Griffiths, A. D. & Tawfik, D. S. Miniaturising the laboratory in emulsion droplets. *Trends Biotechnol.* **24,** 9 (2006).
47. Song, H., Chen, D. L. & Ismagilov, F. Reactions in droplets in microfluidic channels. *Angew. Chem. Int. Ed.* **45,** 7336–7356 (2006).

Acknowledgements

The authors acknowledge financial support from grant CNR-RSTL (Ricerca Spontanea a Tema Libero) no. 3004 'Realizzazione e caratterizzazione di nanostrutture ordinate in cristalli ferroelettrici per la fotonica e studio delle funzionalità' and Grant 'Intesa di programma MIUR/CNR per il Mezzogiorno'.

Author contributions

P.F. and S.G. conceived and designed the experiments. S.C. and V.V. performed the experiments and analysed the data. M.P. and S.C. performed numerical simulations. P.F. and S.G. co-wrote the paper. All authors discussed the results and commented on the manuscript.

Additional information

The authors declare no competing financial interests. Supplementary information accompanies this paper at www.nature.com/naturenanotechnology. Reprints and permission information is available online at http://npg.nature.com/reprintsandpermissions/. Correspondence and requests for materials should be addressed to P.F. and S.G.